Pharmaceutical Research, Vol. 23, No. 4, April 2006 (© 2006)
DOI: 10.1007/s11095-006-9750-6

Research Paper

Osmotic-Driven Release Kinetics of Bioactive Therapeutic Proteins from a Biodegradable Elastomer are Linear, Constant, Similar, and Adjustable

Frank Gu,[1] Ronald Neufeld,[1] and Brian Amsden[1,2]

Received November 11, 2005; accepted December 13, 2005

Purpose. The aim of the study is to determine whether a biodegradable elastomeric device that uses an osmotic pressure delivery mechanism can release different therapeutic proteins at a nearly constant rate in nanomolar concentrations with high bioactivity, given the same formulation conditions. Vascular endothelial growth factor (VEGF) and interleukin-2 (IL-2) were embedded in the device as sample therapeutic proteins, and their release and bioactivity were compared to that achieved previously with interferon-γ (IFN-γ).
Methods. A photo-cross-linkable biodegradable macromer consisting of acrylated star(ε-caprolactone-*co*-D,L-lactide) was prepared. VEGF, IL-2, and IFN-γ were co-lyophilized with serum albumin and trehalose at different ratios and were then embedded into the elastomer by photo-cross-linking the lyophilized particles in a macromer solution. The protein mass and the bioactivity in the release supernatant were measured by enzyme-linked immunosorbent and cell-based assays.
Results. VEGF, IL-2, and IFN-γ were released at the same, nearly constant rate of 25.4 ng/day for over 18 days. Using the optimum elastomer formulation, the release profiles of the proteins were essentially identical, and their rates were linear and constant. Cell-based bioactivity assays showed that 70 and 88% of the released VEGF and IL-2, respectively, were bioactive. The rate of protein release can be adjusted by changing the trehalose loading concentration in the elastomer matrix without altering the linear nature of the protein release kinetics. The elastomeric device degraded in PBS buffer within 85 days.
Conclusions. The elastomer formulation shows promising potential as a sustained protein drug delivery vehicle for local delivery applications.

INTRODUCTION

Over the past two decades, proteins and peptides have become an important class of potent therapeutic drugs. Most protein formulations are administered systemically and are therefore limited by the potential adverse effects of the high plasma concentrations required to achieve an adequate therapeutic efficiency. Many of these proteins act in a paracrine fashion, and thus, the most significant challenge in protein drug delivery is to provide a persistently high dosage at a sustained rate in the vicinity of the target area, which is best accomplished with a zero-order release system. The two major roadblocks to the successful development of implantable protein drug delivery devices are controlling the rate of protein release at a concentration within the therapeutic window and maintaining the bioactivity of the released proteins to maximize the therapeutic effect. To overcome these bariers, polymeric drug delivery systems have been extensively investigated, principally in the form of microspheres (1).

The most widely used biodegradable synthetic polymers for biomedical application are poly(lactide), poly(glycolide), and their copolymer poly(D,L-lactide-*co*-glycolide) (PLGA) microspheres [for review, see (1)]. The mechanism of obtaining a sustained release of entrapped proteins from PLGA microspheres depends on the rate of PLGA degradation. A typical release of macromolecular drugs from PLGA microspheres exhibits triphasic kinetics, which includes a high initial burst release lasting for several hours, followed by a period of low or limited release, and finally a sustained release for the remaining period (2). The initial burst phase is caused by a rapid drug diffusion from the surface of the spheres. In the second phase, the low rate of release is associated with the depletion of the surface drug along with sustained drug release from the erosion of the polymer surface; the third phase is caused by further disintegration providing increased porosity within the microsphere matrix for the final release of the encapsulated drug (2). Several modifications in the PLGA formulations have been made to change the release kinetics from the multiphase to zero- or first-order kinetics. These approaches include the use of

[1] Department of Chemical Engineering, Queen's University, Kingston, Ontario K7L 3N6, Canada.
[2] To whom correspondence should be addressed. (e-mail: amsden@chee.queensu.ca)

ABBREVIATIONS: ASCP, acrylated star copolymer; IFN-γ, interferon-γ; IL-2, interleukin-2; SCP, star copolymer; VEGF, vascular endothelial growth factor.

additives, such as low molecular weight polyglycolic acid (3,4), fatty acid additives (5), or reducing the polymer composition of glycolide (6), or by coating the microspheres with an additional layer of polymer to reduce the initial burst (7). Despite achieving a constant release rate, these approaches also accelerated acid accumulation inside the microsphere because of the nature of the degradation-controlled release mechanism. Consequently, the oligomeric and monomeric products generated as a result of accelerated PLGA degradation can denature the entrapped proteins within 5–8 days (8).

To overcome the drawbacks associated with the erosion-controlled release mechanism, an elastic polymer has been utilized along with osmotic pressure to generate a linear release profile for water-soluble compounds (9–12). In this approach, a constant release rate of a protein can be achieved by distributing protein drugs as lyophilized particles within a rubbery polymer matrix, relying on the osmotic activity of the embedded excipients to drive the protein from the matrix (9). A schematic diagram of the osmotic pressure release mechanism is illustrated in Fig. 1. Upon immersion into an aqueous medium, embedded drug/excipient particles are dissolved by the water diffusing into the polymer and form aqueous microcapsules inside the polymer matrix, thus generating an osmotic activity driving force for further water imbibition into microcapsules containing dissolved drug/excipient particles. Given that the polymer surrounding the microcapsule is elastic, the water imbibition into the microcapsule causes swelling, the extent of which is resisted by the polymer elastic strain. The swelling microcapsules generate cracks because of the bond breakage in the surrounding polymer at a pressure that can be determined by the excipient loading concentration in the elastomer. Provided the particle loading in the polymer matrix is less than the percolation threshold [about 30%, v/v (13)], this swelling and cracking of microcapsules process proceeds in a layer-by-layer fashion throughout the device, and thereby generating a nearly constant release (14,15). Because the osmotic pressure of a saturated excipient concentration at body temperature is much higher than the osmotic pressure of loaded therapeutic proteins (16), the rate of protein release will be driven by the excipient concentration in the polymer. This formulation was initially demonstrated to be capable of delivering proteins of widely different properties from a nondegradable polymer at essentially identical and nearly constant rates (9); however, the osmotic agent used was an inorganic salt, and the bioactivity of the released protein was not assessed.

Previously, we synthesized an elastomeric device by photo-cross-linking an acrylated star copolymer (ASCP) macromer of ε-caprolactone and D,L-lactide (17) and tested the photo-cross-linked elastomer as an interferon-γ (IFN-γ) drug delivery vehicle (16). The protein stability study showed that using trehalose and bovine serum albumin (BSA) co-lyophilized with the IFN-γ as excipients in the elastomer can effectively preserve the bioactivity of the embedded IFN-γ during the photo-cross-linking reaction (16). It was found that IFN-γ can be released from an elastomer slab at a nearly constant rate for up to 3 weeks. The IFN-γ release was driven by the osmotic pressure generated by the dissolved trehalose co-lyophilized with the IFN-γ.

It was the objective of this work to assess whether different therapeutic proteins can be delivered at the same rate via osmotic pressure-driven release from a biodegradable elastomer utilizing the same formulation conditions previously demonstrated for IFN-γ. Thus, two recombinant therapeutic proteins, vascular endothelial growth factor (VEGF) and interleukin-2 (IL-2), were embedded in the biodegradable elastomer matrix using the same IFN-γ formulation (i.e., co-lyophilized with BSA and trehalose in a pH 5 succinate buffer) (16). VEGF and IL-2 represent a class of therapeutic proteins that have a similar range of physical properties to IFN-γ, all of which require a sustained delivery in nanomolar concentrations (Table 1). VEGF and IL-2 are highly potent signaling molecules that have been studied extensively for different clinical applications. VEGF is an angiogenic protein, widely studied for inducing blood vessel growth in ischemic tissues (18). IL-2 is a lymphokine that promotes the proliferation and differentiation of T and B cells and has been extensively tested as a potential drug for cancer treatment (19). Previous studies have suggested that systemic administration such as parenteral injection is unlikely to achieve sufficient therapeutic effects, and localized VEGF delivery is the most efficient treatment for

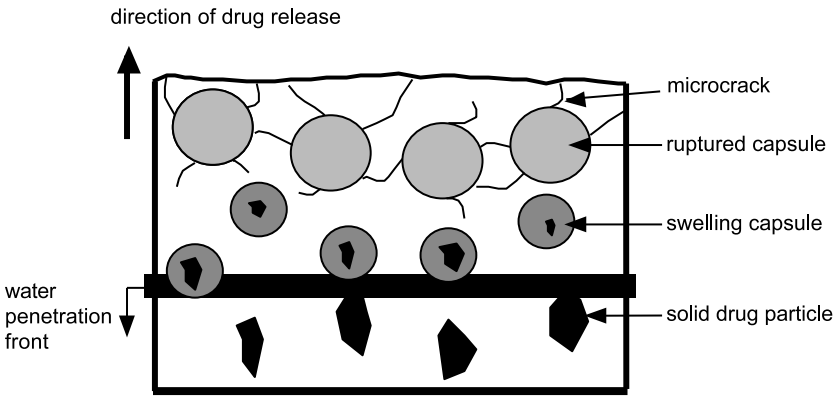

Fig. 1. Schematic of the osmotic pressure-driven release mechanism. There are three zones within the drug-loaded polymer matrix: (1) a zone of microcapsules that have swollen to the fracture point and have created microcracks within the polymer matrix; (2) a zone of microcapsules that are swelling but have not ruptured; and (3) an inner core of dry particles.

Table 1. Biochemical Properties of VEGF, IL-2, and IFN-γ

Protein	MW (kDa)	Bioactive form	pI	Current dosage	Current route of administration
rh-VEGF	38.2 (18)	Dimer (18)	8.5 (18)	5–167 ng/kg (43)	Intracoronary injection (43)
rm-IFN-γ	31.2 (44)	Dimer (44)	8.7 (45)	<50 μg/m^2 (46)	Intravenous injection (46)
rm-IL-2	17.2 (47)	Monomer (47)	8.1 (47)	244 μg/m^2 (48)	Intravenous injection (48)

VEGF = Vascular endothelial growth factor; IL-2 = interleukin-2; IFN-γ = interferon-γ.

ischemia (20). The ideal VEGF delivery system would require 2–3 weeks of localized delivery in the ischemic tissue without any increase at the systemic level (21). Previous studies have examined localized VEGF delivery using PLGA microspheres (8,22–24), calcium alginate beads (23,25), and poly(*N*-isopropylacrylamide) copolymer films (26). Similar rationales for a localized delivery for IL-2 have also been reported. IL-2 is currently administered systemically for treating adult patients with metastatic renal cell carcinoma (27). It was shown that severe toxicity can be induced by the prolonged high doses of systemic IL-2 (28). Previous attempts on localized IL-2 delivery include the use of dextran gels (29), liposomes (30,31), PLGA microspheres (32,33), and HEMA films (34). These studies showed that VEGF and IL-2 can be released for a 1- to 3-week period, but these delivery methods suffered from the rapid initial burst release, low total fraction released, nonlinear release, and rapid protein denaturation within the first week of release. Thus, an optimal delivery vehicle for these therapeutic proteins has not yet been realized.

MATERIALS AND METHODS

Materials

Recombinant human VEGF, murine IL-2, and their corresponding enzyme-linked immunosorbent assay (ELISA) kits were purchased from Peprotech Inc (Ottawa, ON, Canada). The VEGF isoform used in this study is VEGF 165. VEGF 165 is the most abundant and the most biologically active isoform of VEGF family (18,21). EOMA (ATCC CRL-2586) and CTLL-2 (ATCC TIB-214) cells were purchased from American Type Culture Collection (ATCC, Manassas, VA, USA). D,L-Lactide and ε-caprolactone were purchased from Purac (Gorinchem, The Netherlands) and Alfa Aesar (Pelham, NH, USA), respectively. All other reagents and chemicals were purchased from Sigma Aldrich (Oakville, ON, Canada) unless otherwise specified.

Cell Culture

EOMA endothelial cells were cultured in Dulbecco's modified Eagle's medium supplemented with 4 mM L-glutamine, adjusted to contain 1.5 g/L sodium bicarbonate and 4.5 g/L glucose, and 10% fetal calf serum. CTLL-2 lymphoblasts were cultured in RPMI 1640 medium supplemented with 4 mM L-glutamine, 1.5 g/L sodium bicarbonate, 4.5 g/L glucose, 10 mM HEPES, and 2 mM sodium pyruvate, 10% T-STIM with ConA (Catalogue No. 354115, Becton Dickinson, Mississauga, ON, Canada), and 10% fetal bovine serum. Cells were incubated and subcultured according to the procedures recommended by the ATCC.

Polymer Synthesis

The elastomer was prepared as reported previously (17) by photo-cross-linking an ASCP of ε-caprolactone and D,L-lactide (Fig. 2). Briefly, D,L-lactide and ε-caprolactone were polymerized at a molar ratio of 50:50 in the presence of glycerol as the initiator to yield a 7800-g/mol star copolymer. The polymer was then end-capped with acrylate by reaction with acryloyl chloride. The degree of acrylation was confirmed by ^{1}H nuclear magnetic resonance to be 88%.

Device Preparation

Vascular endothelial growth factor and IL-2 were reconstituted with BSA and different ratios of trehalose in a 0.5 mM succinate buffer at pH 5. The protein formulation solution was frozen in liquid nitrogen and was then lyophilized on a Modulyo D freeze dryer (ThermoSavant, Milford, MA, USA) at 80 μbar for 48 h. The lyophilized powder was ground using a mortar and pestle and sieved through a Tyler 100 sieve to yield particles of less than 145-μm diameter, and was then mixed with ASCP polymer solution dissolved in tetrahydrofuran. To make a slab-shaped elastomer, the suspension of lyophilized powder distributed in the ASCP solution was photocured in a rectangular mold (6 × 3 × 1 mm). The amount of trehalose was fixed at 50 and 70% (v/v) of the lyophilized particles. The total volumetric loading of lyophilized particles in the final elastomer matrix was fixed at 10% (v/v) of the elastomer volume.

In Vitro Protein Release and Elastomer Degradation

The release study was carried out by immersing the elastomer slabs in 1 mL of sterile phosphate-buffered saline (PBS) in glass vials placed on a rotary incubator at 37°C and agitated at a rotational speed of 15 rpm. Each release experiment was performed in triplicate, and data were reported as the mean at each time point, with error bars representing the standard deviation. The release medium was replaced with fresh PBS daily to approximate an infinite sink condition. The release medium samples were rapidly frozen in liquid nitrogen and stored at −20°C until immediately prior to the ELISA and bioactivity assays. At each sampling time point, the slabs were blotted dry, then weighed, and the slab dimensions recorded. The VEGF ELISA kit has a very high binding specificity for VEGF; however, it does have high cross-reactivity with VEGF 121 and murine VEGF. Given that neither of these two proteins were present in the release study, it was safe to conclude that the protein detected by the VEGF ELISA kit was exclusively VEGF released from the elastomer device.

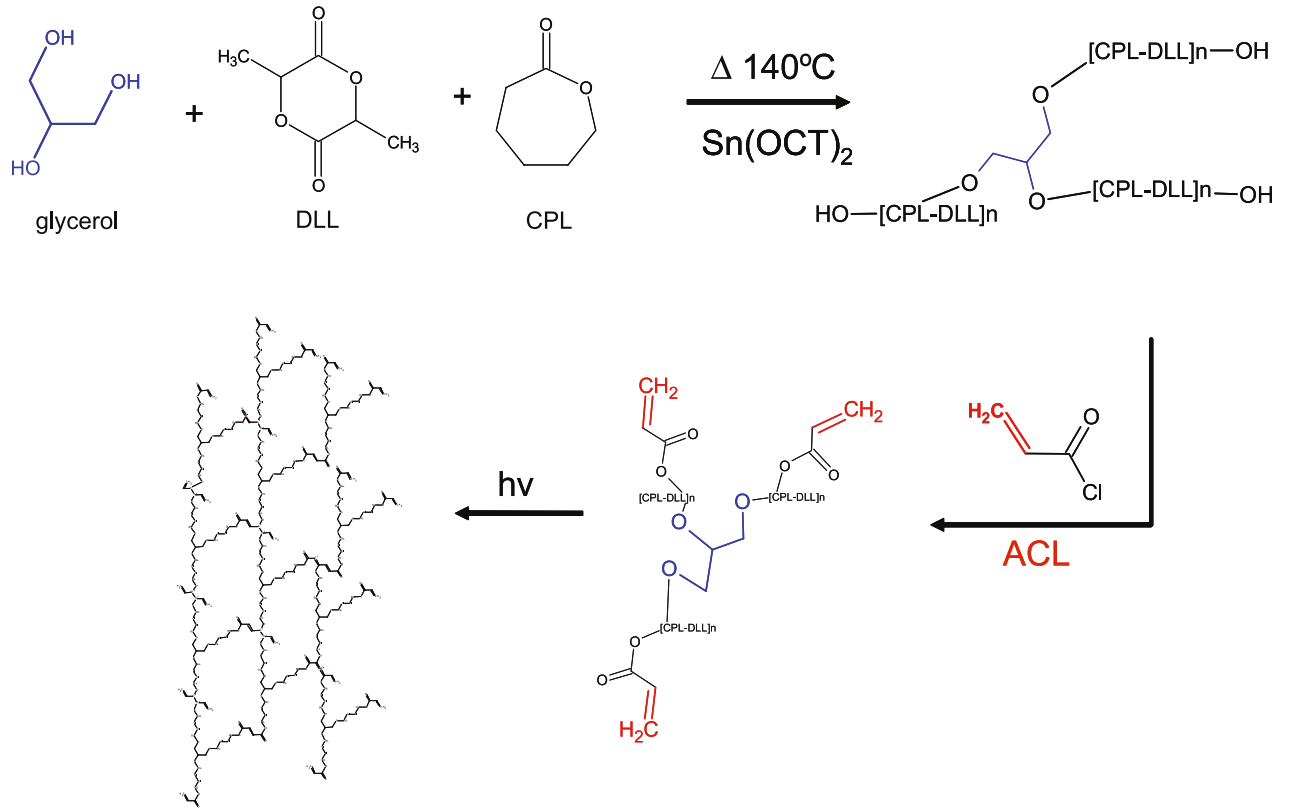

Fig. 2. Elastomer synthesis scheme.

Mass and Bioactivity of the Released Proteins

The concentrations of VEGF and IL-2 in the release medium were measured by using their corresponding ELISA kits. The bioactivities of the released VEGF and IL-2 were measured by their mitogenic activities on EOMA (35) and CTLL-2 cells (36), respectively. Briefly, EOMA and CTLL-2 cells were cultured in a 96-well tissue culture plastic plate (Falcon, Mississauga, ON, Canada) in serum-free and Con-A-free (for the case of CTLL-2 cells) media overnight. The protein release solutions were diluted in serum-free media and added to their corresponding cells and incubated for 24 h. The controls were the diluted release solutions from blank elastomers. The proliferation activity of EOMA and CTLL-2 cells was measured by using an XTT cell proliferation kit II (Roche, Laval, Quebec, Canada). The protein bioactivity reported was normalized by measuring the bioactivity of the freshly reconstituted VEGF and IL-2 after freezing and thawing in the same conditions as for their corresponding samples in the release study.

RESULTS AND DISCUSSION

Protein Release Kinetics

To demonstrate that the elastomer formulation can be used as a vehicle to deliver a variety of therapeutic proteins, VEGF and IL-2 were each examined as candidate drugs. The therapeutic proteins were co-lyophilized with trehalose and BSA. Whereas two different trehalose concentrations were used in the lyophilized particles, the volumetric loading of the total lyophilized solids was fixed at 10% of the elastomer volume to ensure that the total loading was well below the particle percolation threshold, so that osmotic pressure generated by trehalose was the dominant release mechanism (14).

The release profiles of VEGF, IL-2, and IFN-γ are superimposed in Fig. 3. Their release kinetics were essentially identical. For the elastomer slabs containing 50% w/w trehalose in the co-lyophilized particles, VEGF, IL-2, and IFN-γ

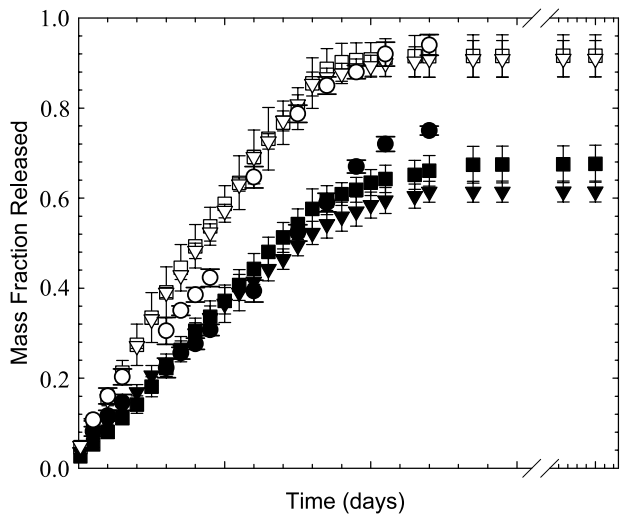

Fig. 3. Release kinetics of vascular endothelial growth factor (VEGF; squares), interferon-γ (IFN-γ; triangles), and interleukin-2 (IL-2; circles) from elastomers containing protein particles co-lyophilized with 50% (closed) and 70% (open) trehalose. The release data of IFN-γ were taken from our previous report (16) and were superimposed on this figure.

were released at an average rate of 16.9 ng/day (or 3.3% of the initial loading mass/day, $R^2 = 0.982$) for an 18-day period (Fig. 3). From days 19 to 21, the average release rate dropped to 5.4 ng/day (or 1.02% of the initial loading mass per day). For the elastomer formulation containing 70% w/w trehalose in the co-lyophilized particles, VEGF, IL-2, and IFN-γ were released at an average rate of 25.4 ng/day (or 4.9% of the initial loading mass per day, $R^2 = 0.982$) for an 18-day period, then gradually decreased to 4.6 ng/day (or 0.83% of the initial loading mass per day) from days 19 to 21. The nearly linear release in both trehalose formulations accounted for over 90% of the total protein released.

The release profiles of the loading excipients BSA and trehalose from both trehalose formulation conditions are shown in Fig. 4, superimposed on the VEGF release profiles. The release rates of BSA, trehalose, and VEGF were essentially identical. The constant protein release in slabs with trehalose particles is supported by the mathematical models describing this osmotic release mechanism (14,15). The faster release kinetics observed from the formulation containing 70% trehalose than those from 50% trehalose can be explained by the greater osmotic activity of trehalose. The osmotic pressure of trehalose and BSA are 98 and 8.6 atm, respectively (16). The osmotic pressure contributed from the embedded therapeutic proteins can be neglected because the therapeutic proteins represent less than 0.001% of the total particle loading concentration in the elastomer. Thus, the 70% trehalose formulation generated a greater driving force of release than the 50% formulation and resulted in a faster protein release.

Bioactivity of the Released Proteins

The bioactivities of VEGF, IL-2, and IFN-γ released from elastomer slabs are shown in Fig. 5. The release media were collected, frozen in liquid nitrogen, and stored at −20°C until immediately prior to the bioactivity assay. The percentage of bioactivity was calculated by taking the cellular response to the active ingredients in the release medium divided by the maximum cellular response of an equivalent concentration of freshly reconstituted protein. The effect of trehalose formulation on protein biological activity after lyophilization is shown in Table 2.

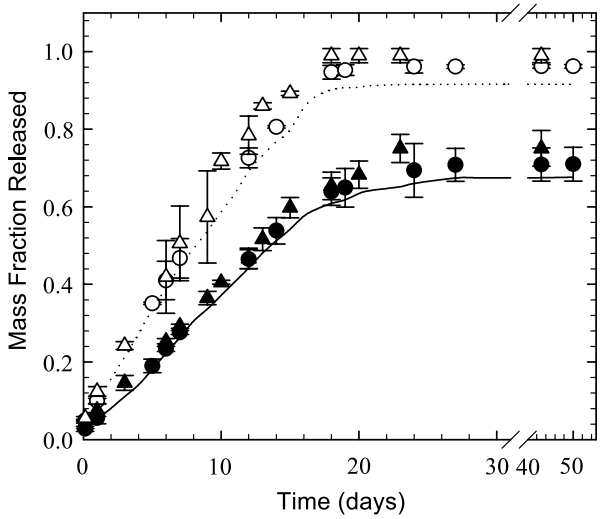

Fig. 4. Release profiles of bovine serum albumin (BSA; circles) and trehalose (triangles) from elastomers containing VEGF/BSA particles co-lyophilized with 50% (closed) and 70% (open) trehalose. The VEGF release is represented by the lines, with the solid and the dashed lines corresponding to the open and the closed symbols of trehalose composition, respectively.

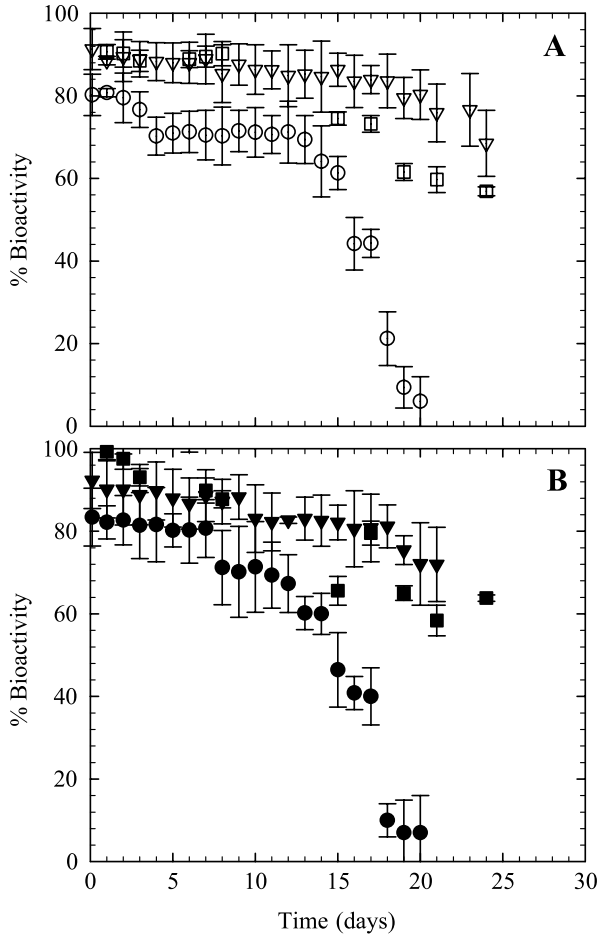

Fig. 5. The bioactivity of the VEGF (circles), IL-2 (triangles), and IFN-γ (squares) released from elastomer slabs. (A) Protein release from elastomers containing protein particles co-lyophilized with 50% trehalose. (B) Protein release from elastomers containing protein particles co-lyophilized with 70% trehalose (closed symbols). The bioactivity data of IFN-γ were taken from our previous report (16) and were superimposed on this figure.

The presence of the excipients greatly improved the stability of VEGF and IL-2 during lyophilization. There was no observable difference between the 50 and 70% trehalose formulations on VEGF and IL-2 bioactivity during lyophilization. The bioactivities of the released proteins from the 50% w/w trehalose formulation are shown in Fig. 5A, and those from the 70% w/w trehalose formulation are shown in Fig. 5B. Whereas VEGF, IL-2, and IFN-γ had essentially the same release kinetics, their bioactivity profiles differed from each other. For the case of VEGF, over 81% of the VEGF released in the first 7 days was bioactive. The fraction of bioactive VEGF decreased to 72% in week 2 and 33% in week 3. The bioactivity of IL-2 was maintained at over 88% during the first week and then gradually dropped to 82 and 76% by the second and third week, respectively. The stability

Table 2. Effect of Trehalose Formulation on VEGF and IL-2 Bioactivity During Lyophilization

	Trehalose formulation		
Protein	No excipient	50%	70%
rh-VEGF	28.3 ± 6.7%	83.3 ± 2.08%	86.1 ± 4.58%
rm-IL-2	41.2 ± 9.8%	82.2 ± 3.6%	87.7 ± 1.15%

profile of IFN-γ was intermediate that of IL-2 and VEGF. There was no influence of trehalose loading concentration on the bioactivities of the three proteins. Because about 80% of the proteins released during the first week of the study were highly bioactive, and the release medium was replaced everyday during the study, it is unlikely that the protein denaturation that occurred in weeks 2 and 3 is a result of the *in vitro* experimental design.

Although the rates of VEGF, IL-2, and IFN-γ release, measured by ELISA, were essentially constant for 18 days, the release windows for the bioactive proteins were shorter. Figure 6 shows the cumulative release of bioactive protein superimposed on their mass release profiles. For the case of VEGF, the rapid decrease of bioactivity on day 14 (Fig. 5A) indicated that virtually all the VEGF released after day 15 was denatured. As shown in Fig. 6, although the mass release of VEGF was detected for over 20 days, the release of bioactive VEGF essentially stopped on day 15. Conversely, the bioactivity of IL-2 was much higher than that of VEGF, and thus the cumulative release of bioactive IL-2 closely followed its mass release.

IL-2 showed high-protein bioactivity throughout the release study, whereas bioactivity of IFN-γ and VEGF decreased after 2 weeks. One possible explanation for the different bioactivity profiles is the effect of disulfide bonds on protein stability. VEGF is a homodimer linked by two disulfide bridges (37), and dimerization is essential for VEGF mitogenic activity (38). IL-2, on the other hand, is bioactive in its monomer form (39). Previous studies have shown that, at low protein concentrations, the disulfide-free proteins or disulfide-containing proteins, whose disulfide bonds are nonessential for protein structure and refolding, generally have a higher tendency to maintain a stable structural confirmation (40). Thus, VEGF would be more prone to denaturation because of the high disulfide nature in the homodimer confirmation. Another explanation for the rapid decrease in VEGF bioactivity on day 12 is associated with acid degradation product accumulation within the device because of elastomer hydrolysis. Previously, we have shown that the pH inside the elastomer was maintained at around 7 for the first 10 days, then gradually dropped below 5 after day 20 (16). It has been demonstrated that the predominant VEGF degradation pathway is the deamidation of Asn-10 residue on the C terminal side (41), and that the rate of deamidation can be greatly accelerated by its adjacent histidine residue when the pH is below 7 (40).

Despite the drop in bioactivity after 14 days for VEGF, the overall bioactive IL-2 and VEGF released from slabs were over 88 and 68%, respectively. These results represent an improvement over previously published results. Using an angiogenesis assay in rats, Richardson *et al.* (24) showed that bioactive VEGF encapsulated in PLGA (85/15) was released

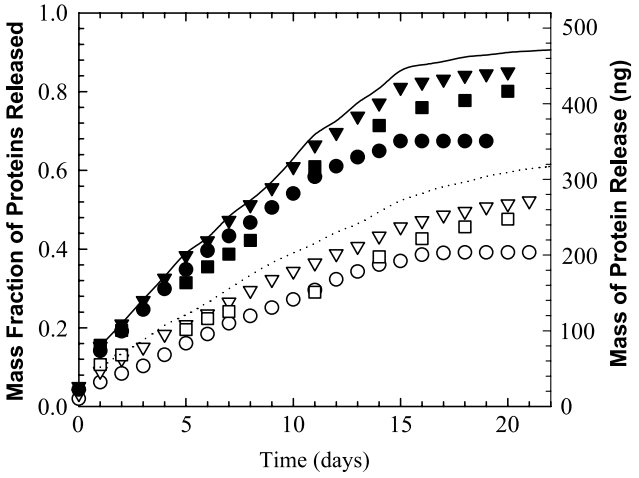

Fig. 6. The cumulative release of bioactive VEGF (squares), IL-2 (triangles), and IFN-γ (circles) from elastomer slabs containing protein particles co-lyophilized with 50% (solid symbols) and 70% (open symbols) trehalose. The lines represent the averaged mass fraction release of VEGF and IL-2, and the solid and the dashed lines correspond to the open and the closed symbols of trehalose composition, respectively. Each point represents the mean of triplicate samples. The standard deviation varied between 5 and 11%.

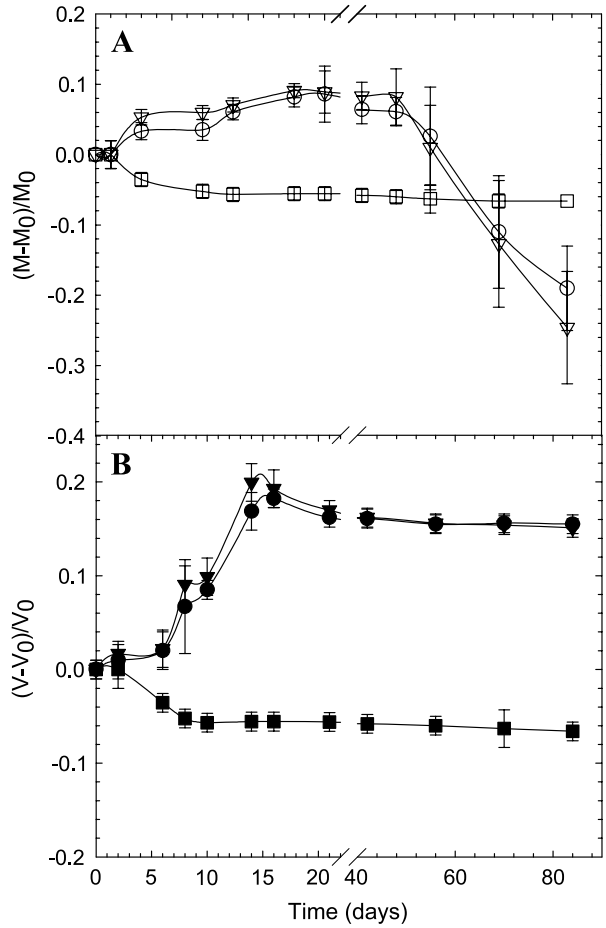

Fig. 7. *In vitro* degradation of elastomer slabs containing protein particles co-lyophilized with 0% (squares), 50% (circles), and 70% (triangles) trehalose. The elastomer slab mass and volume changes are shown in (A) and (B), respectively.

for up to 2 weeks. Cleland *et al.* (8), using an *in vitro* VEGF receptor ELISA, which binds specifically to the receptor domain of VEGF, showed that VEGF released from PLGA (50/50) *in vitro* was stable for up to 8 days. Although the authors showed significant neovascularization induced by the released VEGF, neither study provided a quantitative analysis of the actual percentage of bioactive VEGF released during the study. Sharma *et al.* (42) reported that 40% of IL-2 released from nanospheres made of fumaric and sebacic acids was bioactive after 1 week of release. Thomas *et al.* (32) reported that the bioactivity of IL-2 released from double-emulsion-based PLGA (50/50) formulations was around 80% for the first 5 days, then rapidly dropped to less than 40% by day 10. In our study, protein bioactivity was greatly improved by using osmotic pressure-driven release, which drove protein release before significant elastomer bulk degradation occurred.

Degradation of the Elastomer

To observe the change in elastomer physical properties during and after the release study, the slab mass loss and volume change were measured until the elastomer completely degraded. For the case of elastomers without embedded protein, the elastomer mass decreased by 5% during the first 10 days, then remained constant for the remainder of the study. Elastomers with protein particles, however, showed 10% mass increase in the first 20 days, which dropped rapidly in the eighth week of the degradation study. The change in elastomer dimensions is shown in Fig. 7B. The presence of trehalose increased the elastomer swelling in a dose-dependent manner. For elastomer slabs with embedded protein particles, the swelling ratio gradually increased by 10 and 20% over a 15-day period, and the slabs remained swollen until they degraded (Fig. 7B). The elastomers without excipients shrunk by 10% on day 2 and exhibited no change in volume until the elastomer completely disintegrated.

The greater mass loss and swelling observed in elastomers with embedded particles were a result of the increase in water absorption into the elastomer network (Fig. 1). Previously, we have shown that the 7800-Da ASCP cross-linked elastomer degrades by bulk degradation, the rate of which was largely dependent on the rate of water penetration into the bulk (17). The high osmotic activity of the trehalose accelerated the water diffusion into the elastomer network. The dissolution of the embedded particles in the microcapsules caused the elastomers to undergo swelling. As shown in Fig. 3, most of the protein and trehalose release activity occurred within 20 days, and all the embedded particles were released at a nearly constant rate in the first 2 weeks. From day 20, the slab remained swollen with very little volume change and then rapidly degraded shortly after day 45. Previously, it was shown that the Young's modulus of the elastomer slab decreased in a nearly linear fashion with time after a 4-week incubation period in PBS (17). The osmotic pressure release mechanism requires microcracks in the elastomer to propagate in a layer-by-layer fashion (14), assuming that the protein formulation particles were evenly distributed in the elastomer matrix. Therefore, whereas the trehalose formulation increased the rate of protein release from the elastomer, the microcracks required for the osmotic release caused an extensive increase in surface area for elimination of degradation products from the polymer bulk and accelerated the rate of elastomer degradation. Overall, our degradation study showed that the elastomer slab maintained its physical shape throughout the release period and then degraded slowly after the osmotic-driven release was finished. These results suggest that elastomer slab degradation kinetics are suitable for protein drug delivery applications.

CONCLUSION

Vascular endothelial growth factor and IL-2 were embedded in a biodegradable elastomer via a free radical initiated photo-cross-linking reaction. VEGF and IL-2 were released at near zero-order kinetics for over 18 days, and the rates can be controlled by the loading concentration of trehalose, confirming that the mechanism of release was driven by trehalose osmotic pressure. By applying the same formulation as previously used for IFN-γ release, the release profiles of VEGF, IL-2, and IFN are essential identical, linear, and constant. Released VEGF and IL-2 were highly bioactive during the first 2 weeks of release. The elastomer delivery formulation shows interesting potential as a protein drug delivery vehicle for local protein drug delivery applications.

ACKNOWLEDGMENTS

The authors thank Norma Turner, Dr. Stephen Pang, and Dr. Yat Tse of Queen's University for their assistance. This research was financially supported by the Canadian Institutes of Health Research and the Natural Sciences and Engineering Research Council of Canada.

REFERENCES

1. V. R. Sinha and A. Trehan. Biodegradable microspheres for protein delivery. *J. Control. Release* **90**:261–280 (2003).
2. M. van de Weert, W. E. Hennink, and W. Jiskoot. Protein instability in poly(lactic-*co*-glycolic acid) microparticles. *Pharm. Res.* **17**:1159–1167 (2000).
3. V. Lemaire, J. Belair, and P. Hildgen. Structural modeling of drug release from biodegradable porous matrices based on a combined diffusion/erosion process. *Int. J. Pharm.* **258**:95–107 (2003).
4. H. Sah, R. Toddywala, and Y. W. Chien. Continuous release of proteins from biodegradable microcapsules and *in-vivo* evaluation of their potential as a vaccine adjuvant. *J. Control. Release* **35**:137–144 (1995).
5. W. K. Lee, J. Y. Park, E. H. Yang, H. Suh, S. H. Kim, D. S. Chung, K. Choi, C. W. Yang, and J. S. Park. Investigation of the factors influencing the release rates of cyclosporin A-loaded micro- and nanoparticles prepared by high-pressure homogenizer. *J. Control. Release* **84**:115–123 (2002).
6. D. Sendil, D. L. Wise, and V. Hasirci. Assessment of biodegradable controlled release rod systems for pain relief applications. *J. Biomater. Sci. Polym. Ed.* **13**:1–15 (2002).
7. K. D. Hong, Y. S. Ahn, J. T. Go, M. S. Kim, S. H. Yuk, H. S. Shin, J. M. Rhee, G. Khang, and H. B. Lee. Preparation of double layered nanosphere using dextran and poly(L-lactide-co-glycolide). *Polym-Korea* **29**:260–265 (2005).
8. J. L. Cleland, E. T. Duenas, A. Park, A. Daugherty, J. Kahn, J. Kowalski, and A. Cuthbertson. Development of poly-(D,L-lactide–coglycolide) microsphere formulations containing recombinant human vascular endothelial growth factor to promote local angiogenesis. *J. Control. Release* **72**:13–24 (2001).

9. B. Amsden and Y. L. Cheng. A generic protein delivery system based on osmotically rupturable monoliths. *J. Control. Release* **33**:99–105 (1995).
10. G. Carelli, G. Di Colo, C. Guerrini, and E. Nannipieri. Drug release from silicone elastomer through controlled polymer cracking: An extension to macromolecular drugs. *Int. J. Pharm.* **50**:181–188 (1989).
11. G. Di Colo. Controlled drug release from implantable matrices based on hydrophobic polymers. *Biomaterials* **13**:850–856 (1992).
12. J. Heller, R. W. Baker. *System for Delivering Agent to Environment of Use Over Prolonged Time*, Alza Corporation, USA, 1976.
13. B. G. Amsden and Y. L. Cheng. Enhanced fraction releasable above percolation—threshold from monoliths containing osmotic excipients. *J. Control. Release* **31**:21–32 (1994).
14. B. G. Amsden, Y. L. Cheng, and M. F. A. Goosen. A mechanistic study of the release of osmotic agents from polymeric monoliths. *J. Control. Release* **30**:45–56 (1994).
15. B. Amsden. A model for osmotic pressure driven release from cylindrical rubbery polymer matrices. *J. Control. Release* **93**: 249–258 (2003).
16. F. Gu, H. M. Younes, A. O. El-Kadi, R. J. Neufeld, and B. G. Amsden. Sustained interferon-gamma delivery from a photocrosslinked biodegradable elastomer. *J. Control. Release* **102**: 607–617 (2005).
17. B. G. Amsden, G. Misra, F. Gu, and H. M. Younes. Synthesis and characterization of a photo-cross-linked biodegradable elastomer. *Biomacromolecules* **5**:2479–2486 (2004).
18. N. Ferrara and T. Davis-Smyth. The biology of vascular endothelial growth factor. *Endocr. Rev.* **18**:4–25 (1997).
19. T. Taniguchi, H. Matsui, T. Fujita, C. Takaoka, N. Kashima, R. Yoshimoto, and J. Hamuro. Structure and expression of a cloned cdna for human interleukin-2. *Nature* **302**:305–310 (1983).
20. C. G. Hughes, S. S. Biswas, B. L. Yin, O. V. Baklanov, T. R. DeGrado, R. E. Coleman, C. L. Donovan, J. E. Lowe, K. P. Landolfo, and B. H. Annex. Intramyocardial but not intravenous vascular endothelial growth factor improves regional perfusion in hibernating porcine myocardium. *Circulation* **100**:476 (1999).
21. N. Ferrara, H. P. Gerber, and J. LeCouter. The biology of VEGF and its receptors. *Nat. Med.* **9**:669–676 (2003).
22. T. W. King and C. W. Patrick. Development and *in vitro* characterization of vascular endothelial growth factor (VEGF)-loaded poly(DL-lactic-co-glycolic acid)/poly(ethylene glycol) microspheres using a solid encapsulation/single emulsion/solvent extraction technique. *J. Biomed. Materi. Res.* **51**:383–390 (2000).
23. D. L. Kurdikar and N. A. Peppas. Method of determination of initiator efficiency: application to UV polymerization using 2, 2-dimethoxy-2-phenylacetophenone. *Macromolecules* **27**:733 –738 (1994).
24. T. P. Richardson, M. C. Peters, A. B. Ennett, and D. J. Mooney. Polymeric system for dual growth factor delivery. *Nat. Biotechnol.* **19**:1029–1034 (2001).
25. F. Gu, B. Amsden, and R. Neufeld. Sustained delivery of vascular endothelial growth factor with alginate beads. *J. Control. Release* **96**:463–472 (2004).
26. C. A. Kavanagh, T. A. Gorelova, I. I. Selezneva, Y. A. Rochev, K. A. Dawson, W. M. Gallagher, A. V. Gorelov, and A. K. Keenan. Poly(*N*-isopropy acrylamide) copolymer films as vehicles for the sustained delivery of proteins to vascular endothelial cells. *J. Biomed. Materi. Res. A* **72A**:25–35 (2005).
27. G. Parmiani, L. Rivoltini, G. Andreola, and M. Carrabba. Cytokines in cancer therapy. *Immunol. Lett.* **74**:41–44 (2000).
28. D. M. Pardoll. Paracrine cytokine adjuvants in cancer-immunotherapy. *Annu. Rev. Immunol.* **13**:399–415 (1995).
29. G. W. Bos, J. J. L. Jacobs, J. W. Koten, S. Van Tomme, T. Veldhuis, C. F. van Nostrum, W. Den Otter, and W. E. Hennink. *In situ* crosslinked biodegradable hydrogels loaded with IL-2 are effective tools for local IL-2 therapy. *Eur. J. Pharm. Sci.* **21**: 561–567 (2004).
30. Y. Pellequer, M. Ollivon, and G. Barratt. Formulation of liposomes associated with recombinant interleukin-2: effect on interleukin-2 activity. *Biomed. Pharmacother.* **58**:162–167 (2004).
31. M. V. Backer, R. Aloise, K. Przekop, K. Stoletov, and J. M. Backer. Molecular vehicles for targeted drug delivery. *Bioconjug. Chem.* **13**:462–467 (2002).
32. T. T. Thomas, D. S. Kohane, A. Wang, and R. Langer. Mircoparticlulate formulations for the controlled release of interleukin-2. *J. Pharm. Sci.* **93**:1100–1109 (2004).
33. L. D. Rhines, P. Sampath, F. DiMeco, H. C. Lawson, B. M. Tyler, J. Hanes, A. Olivi, and H. Brem. Local immunotherapy with interleukin-2 delivered from biodegradable polymer microspheres combined with interstitial chemotherapy: a novel treatment for experimental malignant glioma. *Neurosurgery* **52**:872–879 (2003).
34. T. W. Atkins, R. L. Mccallion, and B. J. Tighe. The incorporation and release of glucose-oxidase and interleukin-2 from a bead formed macroporous hydrophilic polymer matrix. *J. Biomater. Sci., Polym. Ed.* **6**:651–659 (1994).
35. N. Ilan, A. Tucker, and J. A. Madri. Vascular endothelial growth factor expression, beta-catenin tyrosine phosphorylation, and endothelial proliferative behavior: a pathway for transformation?. *Lab. Invest.* **83**:1105–1115 (2003).
36. S. Gillis, M. M. Ferm, W. Ou, and K. A. Smith. T-Cell Growth-Factor—Parameters of production and a quantitative microassay for activity. *J. Immunol.* **120**:2027–2032 (1978).
37. Y. A. Muller, H. W. Christinger, B. A. Keyt, and A. M. Vosde. The crystal structure of vascular endothelial growth factor (VEGF) refined to 1.93 A resolution: multiple copy flexibility and receptor binding. *Structure* **5**:1325–1338 (1997).
38. A. J. Potgens, N. H. Lubsen, M. C. van Altena, R. Vermeulen, A. Bakker, J. G. Schoenmakers, D. J. Ruiter, and R. M. de Waal. Covalent dimerization of vascular permeability factor/vascular endothelial growth factor is essential for its biological activity. Evidence from Cys to Ser mutations. *J. Biol. Chem* **269**: 32879–32885 (1994).
39. M. P. Weir, M. A. Chaplin, D. M. Wallace, C. W. Dykes, and A. N. Hobden. Structure activity relationships of recombinant human interleukin-2. *Biochemistry-Us* **27**:6883–6892 (1988).
40. C. Goolcharran, L. L. Stauffer, J. L. Cleland, and R. T. Borchardt. The effects of a histidine residue on the c-terminal side of an asparaginyl residue on the rate of deamidation using model pentapeptides. *J. Pharm. Sci.* **89**:818–825 (2000).
41. C. Goolcharran, J. L. Cleland, R. Keck, A. J. S. Jones, and R. T. Borchardt. Comparison of the rates of deamidation, diketopiperazine formation, and oxidation in recombinant human vascular endothelial growth factor and model peptides. *AAPS PharmSci* **2**:1–6 (2000).
42. A. Sharma, C. M. Harper, L. Hammer, R. E. Nair, E. Mathiowitz, and N. K. Egilmez. Characterization of cytokine-encapsulated controlled-release microsphere adjuvants. *Cancer Biother. Radiol.* **19**:764–769 (2004).
43. T. D. Henry, K. Rocha-Singh, J. M. Isner, D. J. Kereiakes, F. J. Giordano, M. Simons, D. W. Losordo, R. C. Hendel, R. O. Bonow, S. M. Eppler, T. F. Zioncheck, E. B. Holmgren, and E. R. McCluskey. Intracoronary administration of recombinant human vascular endothelial growth factor to patients with coronary artery disease. *Am. Heart J.* **142**:872–880 (2001).
44. M. Fountoulakis, J. F. Juranville, D. Stuber, E. K. Weibel, and G. Garotta. Purification and biochemical characterization of a soluble human interferon gamma receptor expressed in *Escherichia coli*. *J. Biol. Chem.* **265**:13268–13275 (1990).
45. V. Bocci. Physicochemical and biologic properties of interferons and their potential uses in drug delivery systems. *Crit. Rev. Ther. Drug Carr. Syst.* **9**:91–133 (1992).
46. The International Chronic Granulomatous Disease cooperative Study GroupA controlled trial of interferon gamma to prevent infection in chronic granulomatous disease. *N. Engl. J. Med.* **324**:509–516 (1991).
47. K. A. Smith. Interleukin-2—inception, impact, and implications. *Science* **240**:1169–1176 (1988).
48. M. W. Konrad, G. Hemstreet, E. M. Hersh, P. W. A. Mansell, R. Mertelsmann, J. E. Kolitz, and E. C. Bradley. Pharmacokinetics of recombinant interleukin-2 in humans. *Cancer Res.* **50**:2009–2017 (1990).